analytical chemistry

Article

Cite This: Anal. Chem. 2018, 90, 3189−3195

pubs.acs.org/ac

Integration of Inverse Supercritical Fluid Extraction and Miniaturized Asymmetrical Flow Field-Flow Fractionation for the Rapid Analysis of Nanoparticles in Sunscreens

David Müller,*[,†,‡,¶] Margarida Nogueira,[†] Stefano Cattaneo,[†] Florian Meier,[§] Roland Drexel,[§] Catia Contado,[∥] Antonella Pagnoni,[∥] Tjerk de Vries,[⊥] Dror Cohen,[#] Meital Portugal-Cohen,[#] and Andrew deMello[‡]

[†]Centre Suisse d'Electronique et de Microtechnique (CSEM), Bahnhofstrasse 1, 7302 Landquart, Switzerland

[‡]Institute for Chemical and Bioengineering, Department for Chemistry and Applied Biosciences, ETH Zürich, Vladimir-Prelog-Weg 1, 8093 Zürich, Switzerland

[§]Postnova Analytics GmbH, Max-Planck-Strasse 14, 86899 Landsberg am Lech, Germany

[∥]Department of Chemical and Pharmaceutical Sciences, University of Ferrara, Via L. Borsari 46, 44121 Ferrara, Italy

[⊥]Feyecon Carbon Dioxide Technologies, Rijnkade 17a, 1382 GS Weesp, The Netherlands

[#]AHAVA Dead Sea Laboratories, 1 Arava Street, 70150 Lod, Israel

ABSTRACT: We report the use of inverse supercritical fluid extraction (SFE) and miniaturized asymmetrical flow field-flow fractionation (mAF4) for the preparation and subsequent analysis of titanium dioxide nanoparticles in model and commercial sunscreens. The approach allows for the fast and reliable fractionation and sizing of TiO_2 nanoparticles and their quantitation in commercial products. This new method represents a powerful and efficient tool for the verification of nanoparticle content in a wide range of matrixes, as demanded by recently introduced regulatory requirements. Furthermore, the use of carbon dioxide as an environmentally friendly solvent is in line with the increasing need for ecologically compatible analytical techniques.

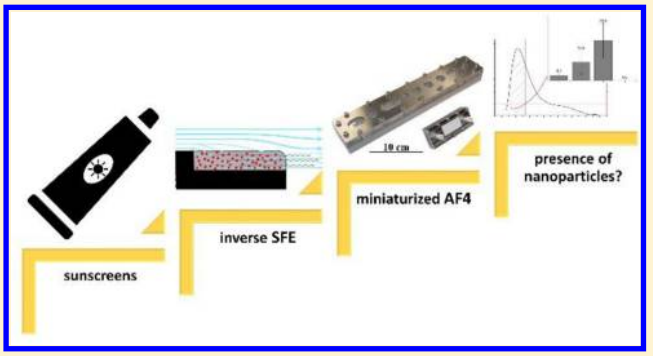

Recently introduced European Union regulations on cosmetic products require that all ingredients present in the form of nanomaterials be clearly indicated as such in the list of ingredients.[1] This requirement calls for the development of comprehensive analytical procedures to ensure manufacturer compliance. The analysis of nanoparticles in complex media, consisting of a complex multicomponent matrix,[2] is a multifaceted challenge involving multiple component processes for sample pretreatment, separation of the engineered nanoparticles (ENPs) from the matrix, separation of nanoparticles on the basis of their size, and chemical analysis. To this end, Wagner et al. recently presented such a categorization in a generic sample preparation scheme for inorganic ENPs within complex matrixes.[3] Such generic procedures, which also integrate appropriate quality criteria to confirm the applicability of the suggested methods, are urgently needed for standardized and systematic development of processes for the separation and analysis of ENPs in complex matrixes. In this respect, the most pressing needs are the development of new analytical techniques for extraction, cleanup, and separation with a view to improving analytical speed, sensitivity, and specificity.[4] One of the most challenging components of the Wagner scheme is the reduction in complexity of the ENP containing sample, either through extraction of nanoparticles from their environment or through simplification of the matrix by removal of excipients that interfere with subsequent analysis. There are several techniques that are frequently used for the isolation of nanoparticles from such matrixes, including acid digestion (assisted by heat, sonication, or microwaves),[3,5−8] colloidal extraction,[3,9] or various treatments with organic solvents.[7,10,11] However, all these processes are complex and time-consuming. Many also completely destroy the particulate nature of the samples, rendering particle size analysis impossible, or have a considerable environmental impact due to the extensive use of harmful solvents.[12,13] Accordingly, the simplification of sample preparation workflows as well as a reduction in solvent requirements, are highly desirable for the analysis of nanoparticle-containing samples.

To this end, we present a novel method for the analysis of TiO_2 nanoparticles in commercial sunscreens, comprising two

Received: November 2, 2017
Accepted: February 7, 2018
Published: February 7, 2018

DOI: 10.1021/acs.analchem.7b04535
Anal. Chem. 2018, 90, 3189−3195

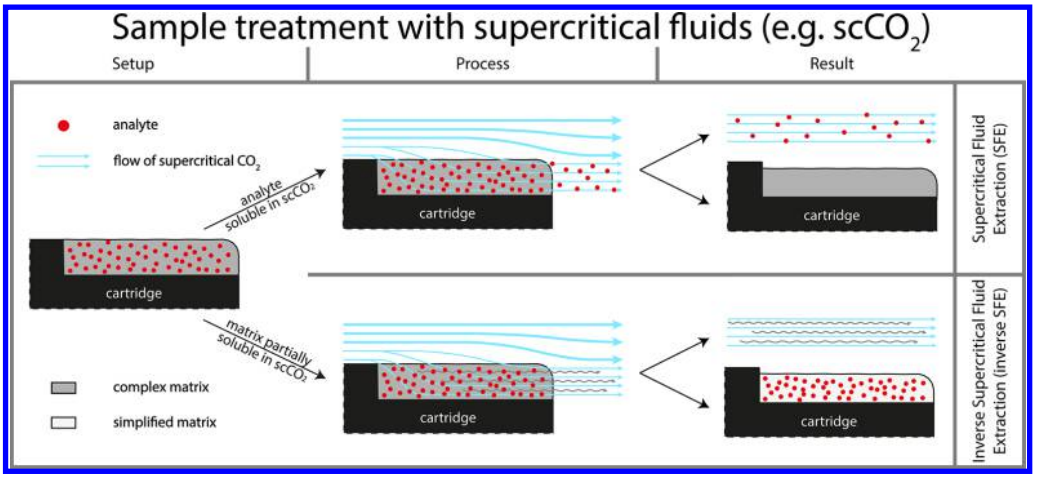

Figure 1. Principles of SFE (top) and inverse SFE (bottom). The setup used for both processes is identical, the primary difference lying in the selection of analyte and matrix and whether the substance of interest is accordingly extracted or left within the simplified matrix.

analytical procedures. We herein propose the use of inverse supercritical fluid extraction (SFE) to simplify complex matrixes containing ENPs while maintaining their particulate nature. To date, the technique of inverse SFE has primarily been used for the isolation of nonpolar pharmaceutical formulations from polar analytes.[13−15] In a recent publication, we presented proof-of-concept experiments that suggested the utility of the technique as a sample pretreatment tool for nanoparticle-containing samples. Specifically, a single model sunscreen was treated and subsequently analyzed by asymmetrical flow field-flow fractionation (AF4) in addition to UV and MALS (multiangle light scattering) detectors and the use of more sophisticated transmission electron microscopy (TEM) analysis.[16] In the present work, we aim to provide a thorough quantitative analysis of several model and commercial sunscreens loaded with ENPs at varying concentrations. In addition to the measurement of processed materials using mAF4, the ENP content was also analyzed using element-specific tools such as inductively coupled mass spectrometry (ICP-MS) and inductively coupled plasma atomic emission spectroscopy (ICP-AES). Field-flow fractionation methods are ideal for such measurements due to the gentle forces used to induce analyte retention and prevent particle alteration.[17] Crucially, the miniaturized AF4 platform reduces both processing times and eluent consumption.[18]

MATERIALS AND METHODS

Samples. *Titanium Dioxide Nanoparticle Standards.* A titanium dioxide (TiO_2)-nanoparticle dispersion, AERODISP W 740 X (40% w/w, EVONIK Industries, Hanau, Germany) was diluted and prepared according to a protocol described elsewhere[16] to yield a final particle concentration of 0.2 mg/mL.

Model Sunscreen. The novel sample preparation method was initially applied to three complex sunscreen models containing different TiO_2 nanoparticle concentrations. Creams were produced individually according to protocols described elsewhere.[16] In the final step, 0.5, 2.5, and 12.5% w/w of a AERODISP W 740 X TiO_2 nanoparticle dispersion (40% w/w, EVONIK Industries, Essen, Germany), as well as the excipients Dow Corning 1503 (Dow Corning Corporation, Midland, MI, United States) and Euxyl PE 9010 (Schülke & Mayr GmbH, Norderstedt, Germany) were added to each cream, resulting in a TiO_2 particle concentration of 0.2, 1.0, and 5.0% w/w, respectively. All creams were homogenized for 5 min at 4000 rpm before being loaded into tubes and stored at room temperature.

Commercial Sunscreens. Five different commercial creams were used to assess our sample preparation method: one cream with a sun protection factor (SPF) of 15 (NiveaCream15), two creams of different brands with a SPF of 30 (GarnierCream30 and NiveaCream30), one cream with an SPF of 50 (CoopCream50), and a sun protection spray with an SPF of 30 (SherpaSpray30). The first three samples contain TiO_2 nanoparticles listed as an ingredient according to European Union legislation, whereas the latter two do not list any nanoparticles as ingredients.

Sample Treatment. Supercritical fluids are well-suited for extraction processes due to their minimal surface tension, low viscosities, and gas-like diffusivities, which allow for thorough sample penetration while maintaining the structure of the residual material.[13] The most obvious choice for the current application is supercritical carbon dioxide ($scCO_2$) because almost all chemical excipients found in emulsion-based cosmetic products are highly soluble in CO_2. $scCO_2$ is chemically inert[19] as well as being nontoxic and nonflammable[20] and is commonly used in the extraction of small and/or nonpolar molecules from natural materials.[21−24] In this regard, common applications include the extraction of essential oils from herbs and spices,[25,26] the removal of caffeine from coffee beans,[27,28] and the extraction and analysis of antioxidants, preservatives, and sunscreen agents in cosmetics.[29,30] In all these applications, however, the analyte itself is soluble in CO_2, with SFE being used to dissolve and remove the analyte from the matrix (upper panel of Figure 1). In this work, however, inverse SFE is used to simplify the matrix by removal of only unwanted components (see lower part of Figure 1). Put simply, the supercritical fluid permeates the matrix, dissolving fatty components and leaving behind a simplified matrix. Once complete, any residual CO_2 is simply removed by lowering the pressure below the critical threshold and returning to ambient conditions. The remaining sample material consists of the polar components of the matrix (e.g., thickening agents) along with any nanoparticles present. Residue can be easily rewetted and subsequently dispersed in an aqueous matrix for subsequent analysis.

DOI: 10.1021/acs.analchem.7b04535
Anal. Chem. 2018, 90, 3189−3195

Supercritical CO_2 Sample Treatment. Details of the analytical method have been described previously,[16] and thus, only the conditions and experimental setup are described herein. For our measurements, the sunscreen was placed on a Teflon cartridge surrounded by a stainless-steel holder. The Teflon part contained a small recess, forming in a cavity with dimensions of 60 × 10 × 0.2 mm and accommodating 100 mg of cream. To ensure a reproducible sample volume, excess sunscreen was removed using a spatula. The Teflon cartridge was then removed from its holder, weighed, and placed in a custom-made extraction vessel. The setup was equipped with a high-pressure CO_2 pump, a pressure/flow regulating system, and a vertically mounted extraction vessel. A custom-made support was used to place two cartridges at once in the extraction vessel. Data indicated no significant difference between each position; however, only the measurements from one cartridge position (closer to the CO_2 inlet) are shown. The sample was then subjected to a constant $scCO_2$ flow of 80 g min^{-1} for 30 min at 40 °C and 131 bar. After extraction, the cartridge was removed and placed in a 15 mL tube for storage. Before the measurement, 10 mL of a solution of 0.2% (v/v) NovaChem (Postnova Analytics GmbH, Landsberg am Lech, Germany) in ultrapure water (Milli-Q, Billerica, United States) was added. NovaChem is a mixture of nonionic and ionic detergents that helps prevent particle agglomeration. The tube was vortexed and sonicated at maximum power (132 kHz) for 30 min using a ultrasonic bath (Ultrasonic Cleaner USC-THD/HF, VWR, Radnor, Pennsylvania, United States) previously cooled to a temperature of 25 °C to further reduce eventual particle agglomerates. All extractions were performed in triplicate (n = 3).

Microwave Assisted Digestion. Between 0.15 and 0.2 g of each sample was deposited in a Teflon vessel (Milestone Inc., Shelton, United States), to which 6 mL of nitric acid (ultrapure p.a. > 65%, Sigma-Aldrich S.R.L., Milano, Italy), 1 mL of H_2O_2 (30% RPE, Carlo Erba Reagents S.r.l., Cornaredo, Italy), and 3 mL of HF (39.5% RPE, Carlo Erba Reagents S.r.l., Cornaredo, Italy) were added. The samples were then digested in the microwave oven (Ethos 900 Milestone, rotor HPR 1000/6M, Milestone Inc., Shelton, United States) according to the following program: 1 min at 250 W and 120 °C, 1 min at 0 W and 120 °C, 5 min at 250 W and 140 °C, 4 min at 400 W and 220 °C, 3 min at 550 W and 220 °C, 5 min at 300 W and 220 °C. The vessel was then left to cool for at least 10 min before it was opened, and 1.5 g of boric acid (99.97% trace metal basis, Sigma-Aldrich S.R.L., Milano, Italy) was added. The solution was then returned into the microwave for 5 min at 300 W. Finally, the vessel was cooled to ambient temperature, and the contents were transferred to a volumetric flask where ultrapure water was added to reach the final volume of 50 mL. All creams dissolved quickly with no visible residue; the final solutions were clear and transparent. All digestions were performed in triplicate (n = 3).

Element-Specific Batch Analysis and Recovery Rate. For the batch-analysis of samples, two different element-specific detectors were used, namely ICP-AES and ICP-MS. For the evaluation of recovery rates, the detected concentrations were compared to those of the samples prepared by direct microwave-assisted digestion (without any treatment by inverse SFE) followed by the corresponding element-specific method. These procedures have previously been shown to allow recovery rates of 98.2 ± 2.2% for the ICP-AES[5] and 101 ± 2% for the ICP-MS.[7]

Inductively Coupled Plasma–Atomic Emission Spectrometry. Titanium determinations were carried out on a PerkinElmer Optima 3100 XL (PerkinElmer Italia S.p.A, Milano, Italy) ICP-AES equipped with an axial torch, segmented array charge-coupled device detector, and Low-Flow GemCone nebulizer with cyclonic spray chamber for sample introduction and choosing, among the several wavelengths, the readings at 337.279 nm. The plasma conditions used were an RF power of 1350 W applied to the plasma and flow rates of 15 L min^{-1} for the plasma gas and 0.5 L min^{-1} for the auxiliary gas with a nebulizer gas flow of 0.65 L min^{-1}. The sample uptake was 1.5 mL min^{-1} for each of 3 replicate scans. The diluted standard solutions were prepared from an elemental standard solution (1000 mg L^{-1} Ti, monoelement standard solution, Carlo Erba, Italy). Titanium quantification limits were evaluated each time from the calibration curves, and the values ranged between 0.54–0.59 mg L^{-1}.

Inductively Coupled Plasma–Mass Spectrometry. Titanium contents were also determined using an Agilent 7900 (Agilent Technologies, Santa Clara, United States) ICP-MS. Sample introduction was carried out with a concentric glass Micromist nebulizer, quartz glass spray chamber and a quartz glass axial torch. A RF power of 1550 W and an argon gas flow of 15 L min^{-1} with a 0.9 L min^{-1} auxiliary gas flow and a carrier gas flow of 1.05 L min^{-1} were used. The sample uptake flow rate was 1.38 mL min^{-1} with a stabilization time of 60 s. The titanium isotopes were recorded with an integration time of 0.5 s. All measurements were performed in triplicate in He-mode to remove polyatomic interferences by introducing a helium flow of 4.3 mL min^{-1} to the collision cell. The calibration was performed with a multielemental standard solution of 1 mg L^{-1} titanium (CPAchem Ltd., Stara Zagora, Bulgaria), and a detection limit of 13 ± 4 μg L^{-1} was obtained according to DIN32645 (calibration curve method). Prior to analysis, all samples were diluted with a 2% (v/v) HNO_3 solution. The isotopes ^{48}Ti and ^{49}Ti were always measured simultaneously. However, only the data from ^{49}Ti are shown.

Miniaturized AF4 with a Multi-Detector Array. *Instrumentation and Carrier Liquid.* Samples treated with inverse SFE were further separated and analyzed using an asymmetrical flow field-flow fractionation system (AF4) from Postnova Analytics GmbH (AF2000 MF, Postnova Analytics GmbH (PN), Landsberg am Lech, Germany), incorporating an autosampler (PN5300), channel thermostat (PN4020), UV (PN3211) and multi-angle light scattering MALS (PN3621, 21 angles) detectors. A miniaturized AF4 cartridge with a tip to tip length of 7 cm (S-AF4-CHA-631, a similar design is further described in ref 18) and incorporating a small 10 kDa regenerated cellulose membrane (20 × 80 mm, Z-AF4_MEM-635–10KD) was used for samples of the model sunscreens and a miniaturized 10 kDa polyether sulfone (PES) membrane (20 × 80 mm, Z-AF4_MEM-631–10KD) for the commercial sunscreens. Furthermore, a 350 μm-thick Mylar spacer was used for all measurements. UV detection was performed at 254 nm, and the measured UV signal was used to correlate concentration with particle size. The MALS detector provided the gyration radius of the particles exiting the miniaturized AF4 (mAF4) separation cartridge (calculated using the random coil model). All presented UV data were collected with the UV detector alone, and all radii of gyration data were determined from the angular dependent light scattering signals obtained via MALS detection. The eluent was prepared using filtrated ultrapure water, to which 0.2% (v/

DOI: 10.1021/acs.analchem.7b04535
Anal. Chem. 2018, 90, 3189–3195

Table 1. Titanium Dioxide Concentrations Measured after Different Sample Treatments and Subsequent Element-Specific Analysis with Model Sunscreens

	sample preparation: microwave digestion				sample preparation: inverse SFE			
	analytical method: ICP-MS		analytical method: ICP-AES		analytical method: ICP-MS		analytical method: ICP-AES	
	conc (%)	SD	conc (%)	SD	conc (%)	SD	conc (%)	SD
model sunscreen, 0.2% TiO_2	0.19	0.02	0.21	0.01	0.25	0.03	0.21	0.03
model sunscreen, 1.0% TiO_2	1.02	0.01	0.99	0.01	1.16	0.05	1.05	0.03
model sunscreen, 5.0% TiO_2	5.17	0.06	4.95	0.07	5.21	0.06	5.3	0.3

v) filtered NovaChem was added. The injection volume was set to 5 μL for the highly concentrated standard TiO_2 nanoparticles, 10 μL for all model sunscreens and the GarnierCream30 (highest TiO_2 content of the commercial samples), and to 20 μL for all other commercial creams. Prior to analysis, the samples from the model sunscreens were diluted 1:4 in a solution of 0.2% (v/v) NovaChem in ultrapure water and then again sonicated at maximum power (132 kHz) for 15 min. Dilution is necessary to prevent overloading effects, which may cause peak shifts and lead to particle agglomeration. The commercial creams were transferred to a glass vial and sonicated for 30 min without further dilution. The temperature of both the autosampler and the channel thermostat were set to 25 °C. Separations and analysis were performed in quadruplicate (m = 4) for each extraction (each cream was sampled in triplicate n = 3) and three out of four measurements per extraction were selected for further investigations. To compensate the baseline drift, UV data was corrected by subtracting a blank run signal measured after injection of pure eluent. For the commercial sunscreens, the baseline corrected UV signal was also divided through the original cream weight, eliminating the influence of different sample amounts. The data acquisition and MALS calculations were performed using the AF2000 Control Unit software (Postnova Analytics GmbH, Landsberg am Lech, Germany), and further evaluations (curve subtractions, etc.) were performed using OriginPro 9.1 (OriginLab Corporation, United States).

Elution Profile. An optimized focusing and elution method was developed to ensure reproducible analysis. The focusing step of the selected elution profile was commenced with a 4 min-long injection flow of 0.15 mL min^{-1} and a cross-flow of 0.30 mL min^{-1}. After a 30 s-long transition time, elution started with a constant cross-flow of 0.30 mL min^{-1} for an additional 30 s, followed by an exponentially decreasing cross-flow (exponent: 0.2), reaching a final value of 0 mL min^{-1} after 30 min. The run was completed with a 10 min long rinsing step to check for additional particle release. To ensure a stable signal, the detector flow rate was maintained at 0.35 mL min^{-1}, with the other flows adjusted accordingly.

Determination of Relative Particle Amounts. For the commercial sunscreens, the relative number of particles with a gyration diameter of less than a 100 nm was estimated by integrating the area under the curve of the UV trace between the end of the void peak (6.25 min) and the elution time corresponding to a gyration diameter of 100 nm, as calculated from the MALS measurements.

RESULTS AND DISCUSSIONS

Method Evaluation with Model Sunscreen. *Recovery Rate.* One of the most relevant figures of merit when separating ENPs from complex matrixes is the recovery rate.[3] This was investigated with ICP-AES and ICP-MS for three model sunscreens that were independently treated with both a standard procedure based on microwave-assisted digestion and inverse SFE.

As shown in Table 1, slightly higher concentrations of TiO_2 were obtained for samples processed with $scCO_2$, resulting in recovery rates of 104 ± 4% for the ICP-AES and 115 ± 17% for the ICP-MS. This apparent increase in concentration is most likely due to solvent evaporation during sample preparation for the inverse SFE treatment: the amount of cream to be processed by $scCO_2$ is weighed after deposition on the Teflon cartridge, where it is spread into a homogeneous 200 μm thin layer to allow thorough sample penetration. In the time between sample deposition and cartridge weighing, the sample is prone to evaporation due the small amount of cream (about 100 mg) and the large exposed surface (600 mm^2). This, in combination with the fact that sunscreens are often tailored for fast solvent evaporation (to promote quick absorption by the skin), may lead to mass losses of up to 10%, shifting the nanoparticle w/w concentration toward higher values. This does not occur when performing acid digestion, thereby explaining the small difference in measured concentrations.

Particle Size Evaluation. Another important factor with regard to the applicability of a sample preparation method is its ability to preserve the size distribution of the nanoparticles and prevent the creation of large agglomerates. To assess this, we used a miniaturized AF4 cartridge to perform rapid size separation and subsequent characterization by different detection techniques.[18] With the miniaturized cartridge and the correspondingly low flow rates, solvent consumption could be reduced to less than 25 mL per run, compared to the 100 mL normally used within the standard analytical channel. The complete run time with the miniaturized channel was 45 min, significantly shorter than what is needed when using standard analytical cartridges, especially when taking into consideration flow presetting and flushing. Besides the three model sunscreens, we also measured the pure nanoparticle dispersion used in their fabrication, allowing direct comparison of the size of the original nanoparticles to those remaining in the simplified matrix after treatment with $scCO_2$. These data are shown in Figure 2, where the solid lines depict the UV fractograms for the different model sunscreens and the black dashed line shows the comparative UV data for the original nanoparticle suspension. The red dashed line shows the averaged MALS curve for the pure dispersion, which is in good agreement with the corresponding curves for the model sunscreens. Peak positions in the different fractograms are in close correspondence with only a small shift of the main peak for the treated particles toward larger sizes. These slight shifts are almost certainly due to aggregation. Nevertheless, because larger particles scatter light strongly, even small amounts of aggregates would result in higher signals. Accordingly, the elugrams indicate the presence of only minor aggregates. The very small peak occurring between 15 and 20 min most likely originates from other cream excipients being slightly active in

DOI: 10.1021/acs.analchem.7b04535
Anal. Chem. 2018, 90, 3189−3195

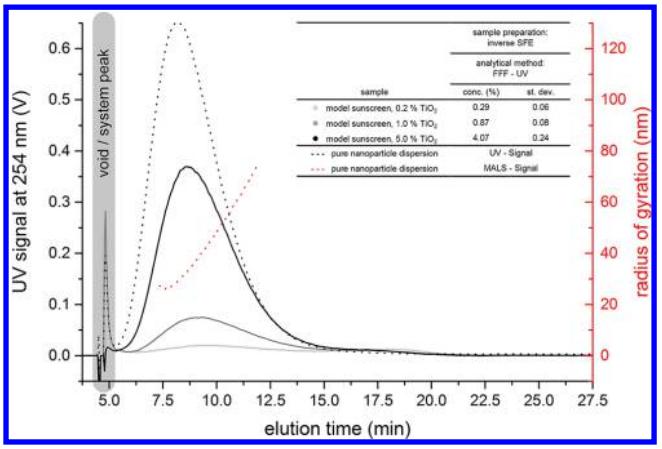

Figure 2. Fractograms of the three $scCO_2$ treated model sunscreens. In addition, the UV signal and calculated radius of gyration from the MALS detector of the pure nanoparticle dispersion are shown, confirming the excellent correspondence between the size distributions from the original particles and those extracted from the complex sunscreen matrix.

the selected UV absorption range, as previously noted[16] and through additional ICP-MS measurements (data not shown). Overall, however, the data clearly indicate excellent preservation of the size distribution of the particles between the pure and treated samples.

Method Evaluation with Commercial Sunscreens. *Recovery Rate.* After the sample preparation efficiency of inverse SFE was thoroughly tested on model sunscreens, the method was applied to commercial sunscreens. For these tests, we purchased a set of five sunscreens and processed them using the same protocol that was used for the three model sunscreen formulations, in addition to microwave-assisted digestion and the treatment with supercritical CO_2 (Table 2). Significantly, the TiO_2 concentrations, determined after microwave digestion with the two methods, are in good agreement, allowing an accurate estimation of the TiO_2 content in the commercial formulations. The values for the CoopCream50 and the SherpaSpray30 (the two creams sold as being TiO_2-free) gave signals consistently below the detection limit of the respective analytical technique.

An interesting result was observed when using elemental techniques to determine the TiO_2 concentration after inverse SFE. The value obtained with ICP-AES was approximately 79% of the initial concentration, with little variation among different screens. Conversely, ICP-MS data estimated 52, 37, and 44% of the corresponding initial values. The reduced recovery rate for the commercial sunscreens may indicate a severe loss of TiO_2 during sample preparation with inverse SFE. However, it has been shown previously that organic acids can form in the presence of water and $scCO_2$ and that such acids can diminish the suspension stability of TiO_2 nanoparticles.[31,32] The treatment with inverse SFE could therefore lead to a modification in the nanoparticle's surfactant properties, which would result in particle agglomeration. These larger aggregates are unlikely to be completely ionized by the ICP ion source, thereby resulting in lower recoveries at the detector. Furthermore, the different measurement process parameters of ICP-MS and ICP-AES such as speed and sample uptake could also yield more rapid precipitation for highly aggregated particles in the case of ICP-MS, leading to lower recovery rates compared to those of ICP-AES.[33]

To further investigate this issue, we performed additional measurements where sunscreens processed using inverse SFE were further treated with microwave-assisted digestion prior to analysis with element-specific tools. This additional mineralization step should allow the proper ionization of all the TiO_2 left after treatment with supercritical CO_2, clarifying whether particles were lost during inverse SFE treatment or not.

The data in Table 3 report the recovery rates for the three nanoparticle-containing commercial samples after employing only inverse SFE and after processing creams with inverse SFE followed by microwave-assisted digestion. As can be seen, the obtained recovery values are higher in the latter case, indicating the issue is not a result of particle loss during inverse SFE but rather due to incomplete ionization of the gently treated samples.

Table 3. Recovery Rates of the Three Commercial Products Containing TiO_2 Nanoparticles[a]

	sample preparation: inverse SFE		sample preparation: iSFE + microwave digestion	
	analytical method: ICP-MS (%)	analytical method: ICP-AES (%)	analytical method: ICP-MS (%)	analytical method: ICP-AES (%)
NC15	52 ± 16	79 ± 4	106 ± 14	95 ± 6
NC30	37 ± 20	78 ± 28	110 ± 8	90 ± 8
GC30	44 ± 7	80 ± 15	68 ± 10	78 ± 12

[a]Abbreviations: NC15, NiveaCream15; NC30, NiveaCream30; GC30, GarnierCream30.

Particle Size Evaluation. The aforementioned drop in recovery rate may pose an issue for quantitative measurements. However, one significant advantage of inverse SFE over microwave-assisted digestion is its capability to preserve nanoparticles during pretreatment, thus allowing further investigation. In the case of microwave-assisted digestion, the metals are fully solubilized, thereby destroying their particulate nature and preventing further investigation. On the contrary,

Table 2. Titanium Dioxide Concentrations Measured after Different Sample Treatments and Subsequent Element-Specific Analysis for Five Commercial Sunscreens

	sample preparation: microwave digestion				sample preparation: inverse SFE			
	analytical method: ICP-MS		analytical method: ICP-AES		analytical method: ICP-MS		analytical method: ICP-AES	
	conc (%)	SD	conc (%)	SD	conc (%)	SD	conc (%)	SD
NiveaCream15	0.99	0.03	0.92	0.01	0.5	0.2	0.72	0.03
NiveaCream30	1.9	0.2	1.76	0.08	0.7	0.4	1.4	0.5
GarnierCream30	3.4	0.2	3.0	0.2	1.5	0.2	2.4	0.4
CoopCream50	<LoD		<LoD		<LoD		<LoD	
SherpaSpray30	<LoD		<LoD		<LoD		<LoD	

DOI: 10.1021/acs.analchem.7b04535
Anal. Chem. 2018, 90, 3189−3195

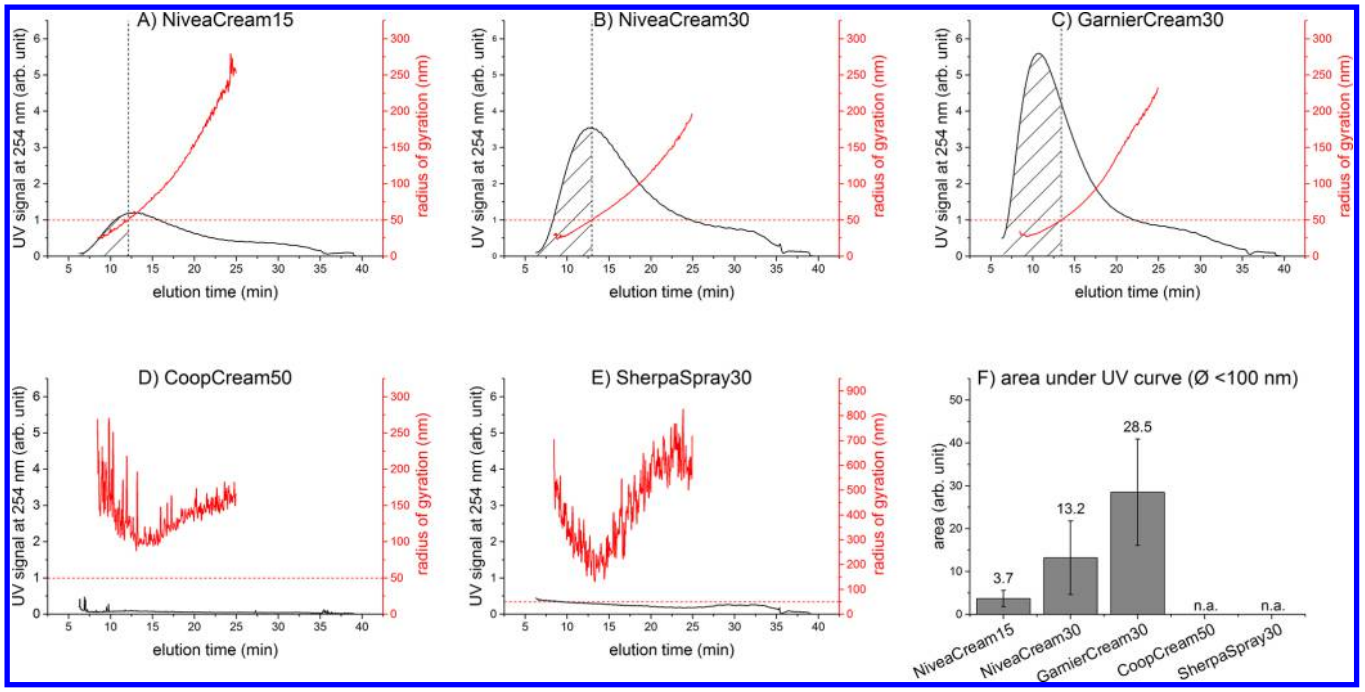

Figure 3. (A–E) Fractograms reporting the UV signal (black) and the calculated radius of gyration (red) for five commercial creams. (A–C) The first three creams clearly contain nanoparticles over a wide size range, whereas the latter two creams (D and E) show limited UV absorption and no detectable particles in the nanoscale range (and an incoherent sizing curve due to low scattering signal). Subset F shows the relative area under the UV curve before the threshold of an averaged gyration radius of 50 nm (dashed area in A–C). Error bars depict standard deviations (n = 9).

Figures 3A–E show the fractograms of resuspensions from the commercial samples treated with supercritical CO_2. In the case of subset A–C, both UV and MALS data show a continuous signal, in line with actual increase in concentration or size and similar to that observed with the model samples. These three creams list, as previously noted, TiO_2 nanoparticles as one of their ingredients. The creams not listing TiO_2 or any kind of nanoparticles show minimal UV absorption. In those cases, the MALS detector is unable to determine a cohesive sizing curve, as the low scattering signal is insufficient to allow fitting to the model (Figures 3D and E). The small UV signal could be due to excipients other than TiO_2 nanoparticles, which may not have been fully removed by inverse SFE and which are also active in the selected UV absorption range.

Figure 3F shows the area under the UV curve for all commercial samples up to a determined diameter of gyration of 100 nm. As the MALS curves for the two later creams, CoopCream50 and SherpaSpray30, never exceed this threshold, no values could be calculated for those samples. Due to the unknown UV absorbance of other cream components and the relatively large deviations between different runs on the same sample (see error bars in Figure 3F), these data cannot be used for an accurate determination of TiO_2 content. Nevertheless, the trends are consistent with the results obtained from the element-specific detection techniques, indicating that the method is eminently suitable for a preliminary screening of TiO_2 particle content.

Inconsistencies in the recovery rate of ICP-MS compared to ICP-AES, as seen here, are generally not uncommon and have been shown to become more severe if different sample pretreatment are employed.[33] In addition to the variations between the different creams, we observed significant deviations between different aliquots of the same sample. This is also indicated by the standard deviations and percentage ranges shown in Tables 2 and 3 as well as the error bars of Figure 3F, which demonstrate the challenging nature of the analysis of the commercial creams compared to model sunscreens. Results could be improved by extending sample preparation by post-treatment stabilization of the sample, as suggested by Wagner.[3] These additional procedures would stabilize the particles and therefore the analytical outcome as a whole as well as optimize method performance for a specific combination and purpose such as iSFE-mAF4-UV-MALS for the determination of TiO_2 particle size distributions or microwave-assisted digestion of the native creams followed by ICP-AES or ICP-MS for the determination of the overall TiO_2 content.

CONCLUSIONS

In this study, we present a novel approach for the analysis of TiO_2 nanoparticles in commercial sunscreens that comprises two analytical procedures. In a first step, inverse SFE was used to gently remove sunscreen matrix components, resulting in dried sunscreen strips containing residual TiO_2 nanoparticles, which were easily redispersible. With recovery rates ranging between 68 and 110%, ICP-MS and ICP-AES measurements of the commercial sunscreen samples before and after treatment confirmed no significant loss of TiO_2 nanoparticles during the sample preparation process.

In a second step, after redispersion in an aqueous solvent, the TiO_2 nanoparticles were characterized using mAF4 hyphenated with UV and MALS detection. This approach allowed for fast and reliable fractionation and sizing of the TiO_2 nanoparticles and thus an unambiguous determination of the presence or absence of TiO_2 particles in commercial sunscreens. The obtained results were in agreement with the data from the element-specific tools and with the label indications for all investigated creams.

DOI: 10.1021/acs.analchem.7b04535
Anal. Chem. 2018, 90, 3189–3195

The combination of inverse SFE with miniaturized AF4 proved to be a highly powerful and efficient tool for the verification of the nanocontent of commercial sunscreens. Due to its wide applicability, this analytical approach is not solely limited to sunscreens but could also be used with cosmetic formulations containing other inorganic particles such as zinc oxide, ceria, or silver. Furthermore, the method is fully in line with the increasingly compelling demand for environmentally friendly analytical methods due to the use of a mild solvent ($scCO_2$) in combination with reduced consumption of eluent. In addition, as a pure sample preparation method, inverse SFE could potentially be applied to other analytical techniques for the investigation of nanoparticles in complex cosmetic matrixes, including electron microscopy, nanoparticle tracking analysis or single particle ICP-MS. This renders inverse SFE a universal tool for the preparation of cosmetic samples, significantly contributing to the quest for routine analytical methods for the verification of European Union nanoparticle labeling requirements.[1]

AUTHOR INFORMATION

Corresponding Author

*E-mail: science@davidmueller.ch.

ORCID

David Müller: 0000-0003-1914-3768

Andrew deMello: 0000-0003-1943-1356

Present Address

¶D.M.: Mythenstrasse 2, 6003 Luzern, Switzerland.

Notes

The authors declare no competing financial interest.

ACKNOWLEDGMENTS

This work was supported by the European Commission Seventh Framework Programme (Project SMART-NANO, NMP4-SE-2012-280779).

ABBREVIATIONS

CO_2	carbon-dioxide
$scCO_2$	supercritical CO_2
AF4	asymmetrical flow field-flow fractionation
mAF4	miniaturized AF4
SFE	supercritical fluid extraction
iSFE	inverse SFE
MALS	multiangle light scattering
ICP-AES	inductively coupled plasma atomic emission spectrometer
ICP-MS	inductively coupled plasma mass spectrometer

REFERENCES

(1) EC. *Off. J. Eur. Union* **2009**, 59−209, DOI: 10.3000/17252555.L_2009.342.eng.

(2) Calzolai, L.; Gilliland, D.; Rossi, F. *Food Addit. Contam., Part A* **2012**, *29* (8), 1183−1193.

(3) Wagner, S.; Legros, S.; Loeschner, K.; Liu, J.; Navratilova, J.; Grombe, R.; Linsinger, T. P. J.; Larsen, E. H.; von der Kammer, F.; Hofmann, T. *J. Anal. At. Spectrom.* **2015**, *30*, 1−11.

(4) von der Kammer, F.; Ferguson, P. L.; Holden, P. A.; Masion, A.; Rogers, K. R.; Klaine, S. J.; Koelmans, A. A.; Horne, N.; Unrine, J. M. *Environ. Toxicol. Chem.* **2012**, *31* (1), 32−49.

(5) Contado, C.; Pagnoni, A. *Anal. Methods* **2010**, *2* (8), 1112−1124.

(6) Dan, Y.; Shi, H.; Stephan, C.; Liang, X. *Microchem. J.* **2015**, *122*, 119−126.

(7) Nischwitz, V.; Goenaga-Infante, H. *J. Anal. At. Spectrom.* **2012**, *27* (7), 1084.

(8) Tadjiki, S.; Assemi, S.; Deering, C. E.; Veranth, J. M.; Miller, J. D. *J. Nanopart. Res.* **2009**, *11* (4), 981−988.

(9) Plathe, K. L.; Von Der Kammer, F.; Hassellöv, M.; Moore, J.; Murayama, M.; Hofmann, T.; Hochella, M. F. *Environ. Chem.* **2010**, *7* (1), 82−93.

(10) Dunford, R.; Salinaro, A.; Cai, L.; Serpone, N.; Horikoshi, S.; Hidaka, H.; Knowland, J. *FEBS Lett.* **1997**, *418* (1−2), 87−90.

(11) Lewicka, Z. a.; Benedetto, A. F.; Benoit, D. N.; Yu, W. W.; Fortner, J. D.; Colvin, V. L. *J. Nanopart. Res.* **2011**, *13* (9), 3607−3617.

(12) Capello, C.; Fischer, U.; Hungerbuhler, K. *Green Chem.* **2007**, *9*, 927−934.

(13) Moore, W. N.; Taylor, L. T. *J. Pharm. Biomed. Anal.* **1994**, *12* (10), 1227−1232.

(14) Messer, D. C.; Taylor, L. T. *Anal. Chem.* **1994**, *66* (9), 1591−1592.

(15) Almodovar, R. A.; Rodriguez, R. A.; Rosario, O. *J. Pharm. Biomed. Anal.* **1998**, *17*, 89−93.

(16) Müller, D.; Cattaneo, S.; Meier, F.; Welz, R.; de Vries, T.; Portugal-Cohen, M.; Antonio, D. C.; Cascio, C.; Calzolai, L.; Gilliland, D.; de Mello, A. *J. Chromatogr. A* **2016**, *1440*, 31−36.

(17) M-M, P.; Siripinyanond, A. *J. Anal. At. Spectrom.* **2014**, *29* (10), 1739−1752.

(18) Müller, D.; Cattaneo, S.; Meier, F.; Welz, R.; DeMello, A. *Front. Chem.* **2015**, *3* (July), 45.

(19) Scalia, S.; Simeoni, S. *Chromatographia* **2001**, *53*, 490−494.

(20) Kaupp, G. *Angew. Chem., Int. Ed. Engl.* **1994**, *33* (14), 1452−1455.

(21) Ndiomu, D. P.; Simpson, C. F. *Anal. Chim. Acta* **1988**, *213*, 237−243.

(22) Hawthorne, S. B. *Anal. Chem.* **1990**, *62* (11), 633−642.

(23) Engelhardt, H.; Zapp, J.; Kolla, P. *Chromatographia* **1991**, *32* (11/12), 527−537.

(24) Reverchon, E.; De Marco, I. *J. Supercrit. Fluids* **2006**, *38* (2), 146−166.

(25) Goto, M.; Sato, M.; Hirose, T. *J. Chem. Eng. Jpn.* **1993**, *26*, 401−407.

(26) Roy, B. C.; Goto, M.; Hirose, T. *Ind. Eng. Chem. Res.* **1996**, *35* (2), 607−612.

(27) Peker, H.; Srinivasan, M.; Smith, J.; McCoy, B. *AIChE J.* **1992**, *38* (5), 761−770.

(28) Tello, J.; Viguera, M.; Calvo, L. *J. Supercrit. Fluids* **2011**, *59* (2011), 53−60.

(29) Lee, M. R.; Lin, C. Y.; Li, Z. G.; Tsai, T. F. *J. Chromatogr. A* **2006**, *1120* (1−2), 244−251.

(30) Scalia, S. *J. Chromatogr. A* **2000**, *870* (1−2), 199−205.

(31) Pettibone, J. M.; Cwiertny, D. M.; Scherer, M.; Grassian, V. H. *Langmuir* **2008**, *24* (13), 6659−6667.

(32) Choi, Y. S.; Nešić, S. *Int. J. Greenhouse Gas Control* **2011**, *5* (4), 788−797.

(33) Iwashita, A.; Nakajima, T.; Takanashi, H.; Ohki, A.; Fujita, Y.; Yamashita, T. *Fuel* **2006**, *85* (2), 257−263.

DOI: 10.1021/acs.analchem.7b04535
Anal. Chem. 2018, 90, 3189−3195